Physica C: Superconductivity and its applications 549 (2018) 102–106

Contents lists available at ScienceDirect

Physica C: Superconductivity and its applications

journal homepage: www.elsevier.com/locate/physc

Accidental degeneracy in *k*-space, geometrical phase, and the perturbation of π by spin-orbit interactions

Philip B. Allen[a], Warren E. Pickett[b,*]

[a] Department of Physics and Astronomy, Stony Brook University, Stony Brook, NY 11794-3800, United States
[b] Department of Physics, University of California Davis, Davis CA 95616, United States

A B S T R A C T

Since closed lines of *accidental* electronic degeneracies were demonstrated to be possible, even frequent, by Herring in 1937, no further developments arose for eight decades. The earliest report of such a nodal loop in a real material – aluminum – is recounted and elaborated on. Nodal loop semimetals have become a focus of recent activity, with emphasis on other issues. Band degeneracies are, after all, the origin of topological phases in crystalline materials. Spin-orbit interaction lifts accidental band degeneracies, with the resulting spectrum being provided here. The geometric phase $\gamma(C) = \pm\pi$ for circuits C surrounding a line of such degeneracy cannot survive completely unchanged. The change depends on how the spin is fixed during adiabatic evolution. For spin fixed along the internal spin-orbit field, $\gamma(C)$ decreases to zero as the circuit collapses around the line of lifted degeneracy. For spin fixed along a perpendicular axis, the conical intersection persists and $\gamma(C) = \pm\pi$ is unchanged.

1. Introduction

A guiding principle of quantum mechanics is that, in the absence of symmetries that allow crossing of eigenvalues as some parameter in the Hamiltonian is varied, the eigenstates will repel due to a non-zero matrix elements of the Hamiltonian and will anticross instead of encountering a degeneracy (eigenvalue crossing). von Neumann and Wigner explored this question [1], finding that only three parameters in a Hamiltonian are necessary for an *accidental* degeneracy (one not enabled by symmetry) to occur; only two are required if the Hamiltonian is real (viz. contains a center of inversion). Bouckaert et al. [2] laid the groundwork for categorizing the symmetry-determined degeneracies in crystalline solids, which is built on crystal symmetry groups and subgroups. Symmetry has persisted in being a fundamental organizing principle in solid state physics.

Following this development, Wigner gave Conyers Herring the task of investigating possible accidental degeneracies in crystalline materials. Among Herring's various findings [3,4] was that not only accidental degeneracies will occur in solids, but that closed lines (loops) of degeneracies are allowed and should not be uncommon. This finding assumed lack of spin-orbit coupling, which is now well known to (primarily) split electronic degeneracies, and occasionally to invert the energies of states. Interest in nodal loops in crystalline spectra has become very active in the last five years, after 75 years of relative neglect (exceptions include Blount [5], Zak [6], Mikitik and Sharla [7–9], and Allen [10,11]).

Separately, a geometric phase in systems undergoing an adiabatic evolution was identified by Berry [12,13], with characteristics tied to degeneracies. Berry introduced the term *diabolical points*, seemingly because degeneracies correspond to points in configuration space where the eigensystem suffers a non-analyticity – diabolical mathematical behavior. His motivation for this term was however ascribed to the conical shape of the energy spectrum around the degeneracy point, the shape being that of a diabolo, the object manipulated by the toy comprised of sticks and strings. Regardless of the etymology, diabolical points and geometric phases have subsequently been identified in numerous systems and occupy a fundamental place in the quantum mechanics of quasiclassical systems.

In this paper we begin by providing the prescription for following, once a degeneracy is located, the degenerate pair around the loop, using modern notation and presenting algorithms explicitly. Such a loop is shown to carry a topological index of $\pm\pi$. Then when SOC is included, as noted in the modern era by Allen [10] and by Burkov et al. [14], the degeneracy is lifted everywhere except possibly at points

* Corresponding author.
E-mail address: pickett@physics.ucdavis.edu (W.E. Pickett).

https://doi.org/10.1016/j.physc.2018.02.024
Received 13 July 2017; Accepted 28 February 2018
Available online 01 March 2018
0921-4534/

where symmetry dictates that matrix elements of the SOC operator vanish. With the non-analyticity of the eigensystem removed, the topological index vanishes, and since all materials possess some SOC, the implication seems to be that the nodal loop is not physical, that it only existed in a SOC-less universe. Straightforward extension of the same thinking to an applied magnetic field leads to the result that the nodal loop can however still be located, though the degeneracy never existed. This paper is concluded by interpreting characteristics of $CaAs_3$, the so-far unique nodal loop semimetal whose only symmetry is inversion, in terms of this formalism.

2. Berry's formalism

More specifically for current purposes, the geometric (or Berry) phase [12] has become a powerful tool for analysis of waves in periodic systems, especially electrons in crystals [6,9,15–18]. The wavevector $\vec{k}$ provides a space in which adiabatic evolution of wavefunctions $\psi_n\left(\vec{k}, \vec{r}\right)$ can be studied, such as by nuclear motion or by applied fields. Singular behavior occurs at band degeneracies where energies $\epsilon_1\left(\vec{k}\right) = \epsilon_2\left(\vec{k}\right)$ are equal and the eigensystem becomes non-analytic. In crystals with inversion symmetry, ignoring spin-orbit interactions, degeneracies occur along closed lines in $\vec{k}$-space [5]. The periodic part $u_n\left(\vec{k}, \vec{r}\right) = \exp\left(-i\vec{k}\cdot\vec{r}\right)\psi_n\left(\vec{k}, \vec{r}\right)$ of ψ is an eigenstate of

$$\mathscr{H}\left(\vec{k}\right) = \left(\vec{p} + \hbar\vec{k}\right)^2/2m + V(\vec{r}). \tag{1}$$

Let the wavevector $\vec{k}(t)$ be given a time evolution which takes it on the closed circuit C, with $\vec{k}(T) = \vec{k}(0)$.

Now suppose that wavefunction evolution is determined by the time-dependent Schrödinger equation with the time-dependent Hamiltonian $\mathscr{H}\left(\vec{k}(t)\right)$. The time-evolution is assumed adiabatic, namely $u_n\left(\vec{k}, \vec{r}, t\right) \propto u_n\left(\vec{k}(t), \vec{r}\right)$. Berry's argument shows that $u_n\left(\vec{k}, \vec{r}, T\right)$ differs from $u_n\left(\vec{k}, \vec{r}, 0\right)$ by the factor $\exp[i\gamma(C, T)]$, where the phase $\gamma(C, T)$ has two parts, $\gamma(C) + \gamma(T)$. The dynamical part $\gamma(T) = -\int_0^T dt\epsilon_n\left(\vec{k}(t)\right)/\hbar$ depends on the time elapsed. The geometric part

$$\gamma(C) = i\oint_C d\vec{k}\cdot\int d\vec{r}\, u_n^*\vec{\nabla}_k u_n \tag{2}$$

is invariant and intrinsic to the circuit and the band properties. In particular, $\gamma(C) = \pm\pi$ if C encloses one (or an odd number) of degeneracy lines. This change of wavefunction sign is familiar from other problems where a circuit of adiabatic evolution surrounds a conical intersection. However, direct evaluation of Eq. (2) is problematic, since wavefunctions must be defined and evaluated in a continuous and single-valued manner. But when the circuit $\mathscr{C}$ is discretized in k-space for numerical integration, the code used for $\psi_n\left(\vec{k}, \vec{r}\right)$ is likely to produce a random phase $\phi_n\left(\vec{k}\right)_i$ that discontinuously jumps to a neighboring $\vec{k}_{i+1}$.

Although gauge invariance is not easy to demonstrate from Eq. (2), Berry gave also an alternate form, for a 3-dimensional parameter space $\vec{k}$, as the flux through a surface S (bounded by C) of a vector $\vec{V}_n$.

$$\gamma(C) = -\int_S d\vec{S}_{\vec{k}}\cdot\vec{V}_n \tag{3}$$

$$\vec{V}_n = \mathrm{Im}\sum_m \frac{\langle n|\vec{\nabla}_{\vec{k}}\mathscr{H}|m\rangle \times \langle m|\vec{\nabla}_{\vec{k}}\mathscr{H}|n\rangle}{\left[\epsilon_m\left(\vec{k}\right) - \epsilon_n\left(\vec{k}\right)\right]^2} \tag{4}$$

The gauge invariance of this vector is easy to demonstrate. Conditions of continuity and single-valuedness of wavefunctions are no longer required. If the circuit surrounds a singularity described by a 2×2 effective Hamiltonian, then the flux equals half the solid angle $\Omega(C)$ subtended in an appropriate scaled space by the circuit as seen from the point of singularity. The appropriate scaled space is the one in which the 2×2 Hamiltonian for states near the conical intersection has the form $\mathscr{H}_{\mathrm{eff}} = \vec{R}\cdot\vec{\sigma}$ in terms of scaled coordinates $\vec{R} = (X, Y, Z)$ and Pauli matrices $\vec{\sigma} = (\sigma_x, \sigma_y, \sigma_z)$. This method will be used twice in this paper. The eigenvalues are $\pm R = \rho_z R$, where the quantum number $\rho_z = \pm 1$ is introduced as a branch index. The geometric phase is then $\gamma(C) = -\rho_z\Omega(C)/2$.

Mikitik and Sharlaĭ [9] provide convincing evidence that the geometric phase $\pm\pi$ is seen experimentally as a shift in the semiclassical quantization condition [19] determining the de Haas-van Alphen oscillations. An extreme experimental case is the shifted quantum Hall oscillations originating from orbits near the Dirac points in graphene [20,21].

The shifts of quantization condition occur for electron orbits (in a $\vec{B}$-field) which surround a degeneracy line (or point, for graphene.) Mikitik and Sharlaĭ also argue [7] that spin-orbit effects can mostly be ignored. This is mostly correct for lighter elements with spin-orbit strength $\xi/\Delta \ll 1$, Δ being any other relevant electron scale such as a band gap. However, the mathematics and the corrections need elucidation. Spin-orbit coupling destroys band degeneracy lines, but it is not evident what happens to the geometric phase of $\pm\pi$.

Mikitik and Sharlaĭ have shown [8] that, in the neglect of SOC, when a cyclotron orbit encircles a nodal line, the areal quantization is shifted, as mentioned earlier. This result is a topological one, depending neither on the form of ϵ_k nor the size or shape of the orbit. This situation occurs for certain orbits in fcc aluminum. Nodal loops were mapped in Al by one of the authors [11] before the recent wider awareness of occurrence of nodal loops. The position of one loop near E_F is shown in

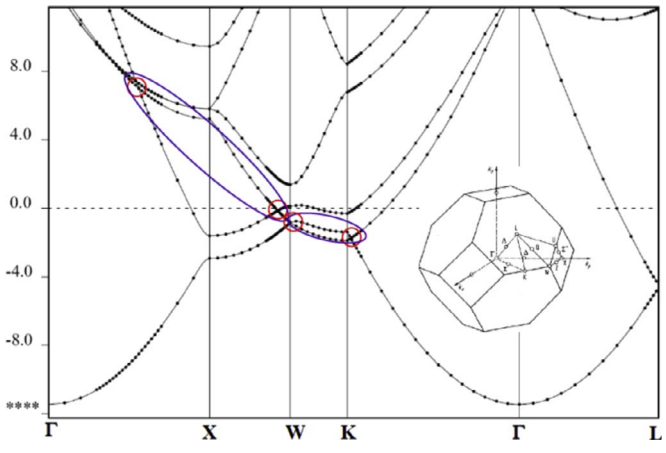

Fig. 1. The band structure of fcc aluminum, with energy in eV. The red circles indicate the important degeneracies, symmetry determined if at a symmetry point, otherwise accidental. On the Brillouin zone in the inset, the blue loops show the approximate positions of the nodal loop, from two viewpoints. (For interpretation of the references to color in this figure legend, the reader is referred to the web version of this article.)

Fig. 1. The locations of the related degeneracies in the electronic spectrum along symmetry lines are also denoted in Fig. 1.

3. Spin-orbit coupling

3.1. Lifting of degeneracy

To see the effect of spin-orbit interactions, add to $\mathscr{H}\left(\vec{k}\right)$ the SOC piece

$$\mathscr{H}_{SO} = (\vec{\sigma}/4m^2c^2)\cdot\vec{\nabla}V\times\left(\vec{p}+\hbar\vec{k}\right). \tag{5}$$

Choose some point $\vec{k}^*$ of accidental degeneracy, and find energies and eigenstates at nearby $\vec{k}$-points using degenerate $\vec{k}\cdot\vec{p}$ perturbation theory. For notational simplicity, $\vec{k}^*$ is the temporary origin of $\vec{k}$. The degenerate basis functions $|1\rangle$ and $|2\rangle$ are the periodic parts u_1 and u_2 at $\vec{k}=\vec{k}^*$. A phase convention is needed; the coefficients C_G of the expansion $u(\vec{r})=\sum C_G\exp(i\vec{G}\cdot\vec{r})$ are chosen real. This requires inversion symmetry, which is hereafter assumed. Each state has two spin orientations, so the effective Hamiltonian matrix is 4×4, with the form

$$\mathscr{H}_{\text{eff}} = \begin{pmatrix} \hbar\vec{k}\cdot\vec{v}_a\hat{1} & \hbar\vec{k}\cdot\vec{v}_b\hat{1}-i\vec{\xi}\cdot\vec{\sigma} \\ \hbar\vec{k}\cdot\vec{v}_b\hat{1}+i\vec{\xi}\cdot\vec{\sigma} & -\hbar\vec{k}\cdot\vec{v}_a\hat{1}\end{pmatrix} \tag{6}$$

where $\hat{1}$ and $\vec{\sigma}$ are 2×2 matrices in spin space. Terms proportional to the 4×4 unit matrix do not mix or split the states and are omitted. The vector $\vec{v}_a$ is half the relative velocity $(\vec{v}_1-\vec{v}_2)/2$, where $\vec{v}_n$ is the band velocity $\vec{\nabla}_k\epsilon_n/\hbar$ at the degeneracy $\vec{k}^*$. The vector $\vec{v}_b$ is the off-diagonal term $\langle2|\vec{p}/m|1\rangle$, which is pure real since C_G is real. The "orbital moment" vector

$$i\vec{\xi} = \langle2|\vec{\nabla}V\times\vec{p}\,|1\rangle/4m^2c^2 \tag{7}$$

is pure imaginary since there is also time-reversal symmetry, under an assumption of no magnetic order or external $\vec{B}$-field. Thus three real vectors, $\vec{v}_a$, $\vec{v}_b$, and $\vec{\xi}$, determine the bands near $\vec{k}^*$. The vector $\vec{\xi}$ is a close analog to angular momentum, hence the designation as orbital moment. Consider a system with two degenerate p-states $|x\rangle$ and $|y\rangle$. The angular momentum operator $\vec{L}$ has an imaginary off-diagonal element. The mixed states $|x\rangle\pm i|y\rangle$ are eigenstates of $\vec{L}$ with $\langle\vec{L}\rangle=\pm m\hbar\hat{z}$. The magnitude m deviates from 1 if the point symmetry is less than spherical.

First suppose that $\vec{\xi}=0$. Since $\vec{v}_a$ and $\vec{v}_b$ are not generally collinear and provide the directions along which matrix elements of $\mathscr{H}_{\text{eff}}$ vary, they define a direction of $\vec{k}$, namely $\vec{v}_a\times\vec{v}_b$, along which $\mathscr{H}_{\text{eff}}=0$. This is the *direction of the line of degeneracy*. After allowing $\vec{\xi}\neq0$, eigenvalues of Eq. (6) are $\pm\lambda$ where

$$\lambda = \sqrt{\kappa_a^2+\kappa_b^2+\xi^2} \tag{8}$$

with $\kappa_a=\hbar\vec{k}\cdot\vec{v}_a$, $\kappa_b=\hbar\vec{k}\cdot\vec{v}_b$, and $\xi=|\vec{\xi}|$. Each eigenvalue belongs to a Kramers doublet of two opposite spin states. The original degeneracy (without spin-orbit interaction) of 2 (neglecting spin) or 4 (including spin) is lifted everywhere unless $\vec{\xi}=0$. This should happen only at isolated points in the Brillouin zone, not coinciding with degeneracy lines $\vec{k}^*$. No accidental degeneracies remain, but Kramers degeneracy occurs everywhere. Bands near $\vec{k}^*$ are shown in Fig. 2.

3.2. Geometric phase

The geometric phase under consideration involves a circuit $C\left(\vec{k}\right)$ surrounding the $\vec{k}^*$ line. A circular path in two-dimensional (κ_a,κ_b)-space, namely $C=(\kappa\cos\phi,\kappa\sin\phi)$, $0\to\phi\to2\pi$ is the simplest realization. To calculate $\gamma(C)$, separate Eq. (6) into two similar 2×2 submatrices by choosing basis states with spins polarized along $\vec{\xi}$, which will be used as the z-axis of spin space. The submatrices are

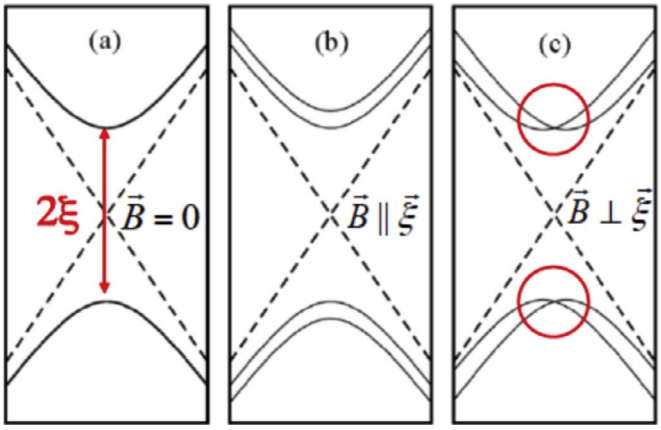

Fig. 2. Energy *versus* $\left|\vec{k}\right|$ near the degeneracy point, for (a) no magnetic field, the gap is 2ξ, (b) field parallel to $\vec{\xi}$, and (c) field perpendicular to $\vec{\xi}$, with the degeneracies emphasized. The dashed lines are for $\xi=0$ and $b=0$; solid lines in panel (a) are $\pm\lambda$, which becomes $\pm\xi$ at the degeneracy point $\vec{k}=0$.

$$\mathscr{H}^{\pm}_{\text{eff}} = \begin{pmatrix} \kappa_a & \kappa_b\mp i\xi \\ \kappa_b\pm i\xi & -\kappa_a\end{pmatrix}, \tag{9}$$

where the upper sign goes with spin up, $\sigma_z=1$.

The circuit can now be considered as a path $C\left(\vec{\lambda}\right)$ in a 3-d $\vec{\lambda}$-space, where $(\lambda_x,\lambda_y,\lambda_z)=(\kappa_b,\sigma_z\xi,\kappa_a)$. On this circuit, λ, κ, and ξ are all constant. The effective Hamiltonian has the desired scaled form. The solid angle is $\sigma_z2\pi(1-\xi/\lambda)$, so the geometric phase is

$$\gamma(C) = -(\Lambda_z\sigma_z)\pi(1-\xi/\lambda). \tag{10}$$

where $\Lambda_z=\pm1$ is the branch index. This is *one of the two main results* of this section. It shows how spin-orbit splitting destroys the simple phase of $\pm\pi$ when the circuit has such a small radius that $\xi\sim\lambda$. If spin-orbit interaction is weak, it does not need a large orbit to have $\xi/\lambda\ll1$ and approach the full simple phase of $\pm\pi$.

3.3. The rest of the story

This is not the full story. Analogous to the lack of phase of u_k not being defined by the Schrödinger equation, the choice to evolve at fixed σ_z was arbitrary. The states of Kramers doublets can be mixed by arbitrary unitary transformations. Evolution of a doublet around a circuit introduces not a simple geometric phase, but a unitary matrix. The $\gamma(C)$ phases just computed are actually the diagonal elements $\exp(\pm i\gamma(C))$ of a 2×2 unitary matrix in the representation with spin quantized along $\vec{\xi}$. It will emerge below that this is indeed the correct adiabatic evolution of the Kramers doublet when a small magnetic field is imposed along the $\vec{\xi}$ direction.

Berry's original argument assumed that $\mathscr{H}$ had a discrete spectrum along C. There is a physically natural way to retain this. Magnetic fields are used to generate cyclic evolution in $\vec{k}$-space. Magnetic fields also lift Kramers degeneracy. The simplest theoretical device is to add to $\mathscr{H}_{\text{eff}}$ a Zeeman term $\mathscr{H}_Z=-\vec{b}\cdot\vec{\sigma}$ coupling only to spin.

To proceed further, an explicit representation of eigenstates is needed. Eigenstates of the effective Hamiltonian (9), labeled by energy $\pm\lambda$ and $\sigma_z=\uparrow,\downarrow$ are chosen as

$$|s\rangle = |-\lambda,\uparrow\rangle = \frac{1}{n}\begin{pmatrix} -\kappa_b + i\xi \\ \kappa_a + \lambda \end{pmatrix} \otimes |\uparrow\rangle, \tag{11}$$

$$|t\rangle = |-\lambda,\downarrow\rangle = \frac{1}{n}\begin{pmatrix} -\kappa_b - i\xi \\ \kappa_a + \lambda \end{pmatrix} \otimes |\downarrow\rangle, \tag{12}$$

$$|u\rangle = |+\lambda,\uparrow\rangle = \frac{1}{n}\begin{pmatrix} \kappa_a + \lambda \\ \kappa_b + i\xi \end{pmatrix} \otimes |\uparrow\rangle, \tag{13}$$

$$|v\rangle = |+\lambda,\downarrow\rangle = \frac{1}{n}\begin{pmatrix} \kappa_a + \lambda \\ \kappa_b - i\xi \end{pmatrix} \otimes |\downarrow\rangle. \tag{14}$$

These are written as the direct product of spatial times spin two-vectors. The normalization is $n = \sqrt{2\lambda(\lambda + \kappa_a)}$. As long as ξ is non-zero, $1/n$ is non-singular and these are smooth, single-valued functions of (κ_a, κ_b), unique except for an arbitrary overall phase, which cannot alter $\gamma(C)$. The lower Kramers doublet $|s\rangle$, $|t\rangle$ has "orbit moments" $\langle i|\vec{\nabla} V \times \vec{p}\,/4m^2c^2|i\rangle = \mp(\xi/\lambda)\vec{\xi}$ oriented antiparallel to spin, while the upper Kramers doublet $|u\rangle$, $|v\rangle$ has identical orbit moments except oriented parallel to spin.

Now the Zeeman term is added. Diamagnetic coupling is neglected. Without loss of generality, the part of the field $\vec{B} = \vec{b}/\mu_B$ perpendicular to ξ can be used to define the x direction of spin. The total Hamiltonian in the basis $|s\rangle$, $|t\rangle$, $|u\rangle$, $|v\rangle$ is

$$\mathscr{H}_{\rm tot} = -\begin{pmatrix} \lambda + b_z & \frac{\kappa}{\lambda}b_x e^{i\omega} & 0 & i\frac{\xi}{\lambda}b_x \\ \frac{\kappa}{\lambda}b_x e^{-i\omega} & \lambda - b_z & -i\frac{\xi}{\lambda}b_x & 0 \\ 0 & i\frac{\xi}{\lambda}b_x & -\lambda + b_z & \frac{\kappa}{\lambda}b_x e^{-i\omega} \\ -i\frac{\xi}{\lambda}b_x & 0 & \frac{\kappa}{\lambda}b_x e^{i\omega} & -\lambda - b_z \end{pmatrix} \tag{15}$$

The factor $(\kappa/\lambda)\exp(i\omega) = \langle s|\sigma_+|t\rangle$ introduces the new angle ω

$$e^{i\omega} = \frac{\lambda}{\kappa} - \frac{\xi(\xi - i\kappa_b)}{\kappa(\lambda + \kappa_a)}. \tag{16}$$

As the circuit C is followed (ϕ going from 0 to 2π, with ξ, κ, λ constant), ω also evolves from 0 to 2π.

If the field $\vec{b}$ is along z, the upper and lower Kramers doublets are not coupled. The degeneracy is lifted everywhere, and adiabatic evolution proceeds smoothly on the resulting non-degenerate states, yielding the phases $\gamma(C)$ of Eq. (10). The previous discussion was correct. The result Eq. (10) can also be obtained directly from Eq. (2) using Eqs. (11)–(14). For fields perpendicular to z, there is both intra- and inter-doublet spin mixing, according to Eq. (15). To first order, since $\vec{b} \ll \lambda$, inter-doublet mixing terms $\pm i\xi b_x/\lambda$ can be neglected, giving 2×2 effective Hamiltonian matrices, of the form

$$\mathscr{H}_{\rm eff}\left(\vec{b}\right) = \lambda_z \lambda \hat{1} - \begin{pmatrix} b_z & \frac{\kappa}{\lambda}b_x e^{i\lambda_z\omega} \\ \frac{\kappa}{\lambda}b_x e^{-i\lambda_z\omega} & -b_z \end{pmatrix} \tag{17}$$

The eigenvalues are

$$\pm\lambda \pm \mu \quad \text{where } \mu^2 = b_z^2 + \frac{\kappa^2}{\lambda^2}b_x^2 \tag{18}$$

These eigenvalues have an interesting feature: at the degeneracy point $\kappa = 0$, in the center of circuit C, $\mu = 0$ and Kramers degeneracy is **not** lifted, provided $\vec{b}$ is perpendicular to $\vec{\xi}$. The states at $\vec{k}^*$ have anisotropic g factors which vanish in two directions. The vanishing Zeeman splitting means that a conical intersection, hidden unless $\vec{b} \neq 0$, exists exactly where the original band intersection (for $\xi = 0$) was located. This also yields a simple geometrical phase of $\pm\pi$. Bands for $\vec{b} \| \vec{\xi}$ and $\vec{b} \perp \vec{\xi}$ are shown in Fig. 2 panels (b) and (c).

A full calculation of $\gamma(C)$ for the 4 new eigenstates of Eq. (15) is difficult. The Berry method of solid angle works when the basis functions $|1\rangle$, $|2\rangle$ of the 2×2 effective Hamiltonian are fixed at $\vec{k}^*$, whereas the basis functions $|s\rangle$, $|t\rangle$ or $|u\rangle$, $|v\rangle$ used in Eq. (17) depend on $\vec{k}$. However, the most important limit remaining to be resolved is when the circuit radius κ is small relative to spin-orbit splitting ξ. In this limit, the basis functions lose their $\vec{k}$-dependence. The relevant scaled parameters are $\vec{\mu} = ((\kappa/\lambda)b_x\cos\omega, -\lambda_z(\kappa/\lambda)b_x\sin\omega, b_z)$. The circuit parameterized by ϕ is equally well parameterized by ω which evolves from 0 to 2π. The solid angle in $\vec{\mu}$-space is $2\pi\Lambda_z(1 - b_z/\mu)$, so the geometric phase is

$$\gamma(C) = -\pi\beta_z\Lambda_z\left(1 - \frac{b_z}{\sqrt{b_z^2 + (\kappa/\lambda)^2 b_x^2}}\right), \tag{19}$$

where (Λ_z, β_z) are the two branch indices in the eigenvalue $\pm\lambda \pm \mu = \Lambda_z\lambda + \beta_z\mu$. This is the *other main result* of this section. If $b_z = 0$, the full geometric phase $\gamma(C) = \pm\pi$ is restored no matter how small the circuit radius. Even though the degeneracy was lifted by spin-orbit interactions, the hidden conical intersection exposed by a Zeeman field controls the result. The nodal loop can be located and followed, though it never existed.

4. Connections to the lowest symmetry nodal line semimetal

Reports of identification of nodal loops in electronic structures took off in 2014. There had been an early report in 2009, before widespread recognition of nodal loops resulted from the 2011 paper of [14]. These authors popularized nodal loop semimetals in the context of topological semimetals (primarily Weyl semimetals), pointing out several general features. The earlier report of [22] involved a nodal loop comprised of a pair of coinciding Fermi rings, making it a circular nodal ring coinciding with the Fermi energy E_F, a simple but remarkable coincidence. The system was a compensated semimetal of ferromagnetic nanolayers of $SrVO_3$ quantum confined within insulating $SrTiO_3$. Mirror symmetry was a central feature: two bands having opposite reflection symmetries crossed in the mirror plane, making it a nodal loop enabled by symmetry (thus not purely accidental).

What is unlikely but not statistically improbable is: (1) having the nodal loop cut by E_F while (2) the remainder of the Brillouin zone is gapped. Such loops will have real impact, and possibly unusual boundary properties, when they are the sole bands around E_F. This coincidence with E_F occurred for the ferromagnetic $SrVO_3$ nanolayer mentioned above. Crystal symmetry has played an important role in nearly all nodal loop families discovered so far. The enabling symmetries include screw axes [23], mirror symmetries [14,22–27], as well as the much studied TaAs class that has no center of inversion [28–35].

Herring [3,4] however pointed out that inversion symmetry $\mathscr{P}$ alone is sufficient to allow nodal loops of degeneracies (fourfold: two bands times two spins), a result extended recently [14,23]. This is easy to understand: $\mathscr{P}$ symmetry leads to a real Bloch Hamiltonian $H\left(\vec{k}\right)$ if the center of inversion is taken as the origin. The minimal (for each spin) 2×2 Hamiltonian then has the form $H\left(\vec{k}\right) = f_k\tau_x + g_k\tau_z$ (neglecting spin degeneracy for the moment) with real functions f_k, g_k; $\vec{\tau}$ represents the Pauli matrices in orbital space. Degeneracy of the eigenvalues $\varepsilon_k = \pm(f_k^2 + g_k^2)^{1/2}$ requires $f_k = 0 = g_k$, two conditions on the 3D vector $\vec{k}$ giving the necessary flexibility to arrange degeneracy. Allen has given a constructive prescription [10] for mapping the nodal loop once a degeneracy is located.

The Zintl semimetal $CaAs_3$, which has $P\bar{1}$ symmetry (inversion only) has been shown [36] to have, before SOC is considered, a nodal loop that is cut by the Fermi energy four times. It and its three isovalent triarsenide sisters (Ca → Sr, Ba, Eu) were synthesized more than thirty years ago, with their structure, transport, and optical properties studied

by von Schnering, Bauhofer, and collaborators [37,38].

$CaAs_3$ is unique in a few ways. It sports a single nodal loop. Already Herring had noted that three classes were possible: single nodal loops, loops that occur in pairs, and loops that are extended into neighboring zones, being "closed" by the periodicity of k space. Other than these tri-arsenides, nodal loop semiconductors all have pairs of nodal loops imposed by their crystal symmetry. $CaAs_3$ also is the sole triclinic ($P\bar{1}$) member of this family of tri-arsenides [37]. $CaAs_3$ also has the accidental feature that the SOC splitting of the nodal loop ΔE_{soc} (arising from the As SOC) is very similar to its small dispersion of 30–40 meV around the loop. This similarity of energy scales leaves the resulting band structure on the borderline between remaining a nodal loop semiconductor or moving into the realm of extremely small gap nodal insulator; this distinction is too small for present DFT calculations to give conclusive statements about. Recall also that such small gap systems are unstable to excitonic condensation.

Thus $CaAs_3$ presents a unique nodal semimetal amongst those discovered and studied so far. Unfortunately, $CaAs_3$ samples are heavily twinned due to a structural transition between the growth temperature and the temperatures of interest (room temperature and below). The twin boundaries likely produce carriers that will complicate interpretation of transport and spectroscopic data. The results of Sec. III point out the conceivability of identifying the nodal loop even though it has been destroyed by spin-orbit coupling. The experimental challenge is constructing and experimental realization of the theoretical "SQUID loop" – the circuit $\mathscr{C}$ – that enables detection of the loop of degeneracies. This possibility provides impetus for discovering, or designing, other nodal loop semimetals with minimal symmetry.

Acknowledgments

P.B.A. thanks A. G. Abanov and M. S. Hybertsen for assistance, and also thanks the Stony Brook students of 2007 Phy556 who were subjected to preliminary versions of the formalism presented in this work. W.E.P. acknowledges collaboration with Y. Quan and T. Siegrist on $CaAs_3$.[36] P.B.A was supported earlier by NSF grant no. NIRT-0304122 and currently by DOE grant DE-FG02-08ER46550. W.E.P. was supported by DOE grant DE-FG02-04ER46111.

References

[1] J. von Neumann, E.P. Wigner, On the behavior of eigenvalues in adiabatic processes, Physik. Z. 30 (467) (1929) 167. Translated in R. S. Knox and A. Gold, Symmetry in the Solid State (Benjamin, New York, 1964).
[2] L.P. Bouckaert, R. Smoluchowski, E.P. Wigner, Theory of Brillouin zones and symmetry properties of wave functions in crystals, Phys. Rev 50 (58) (1936).
[3] W.C. Herring, Accidental degeneracy in the energy bands of crystals, Phys. Rev 52 (365) (1937).
[4] W.C. Herring, On Energy Coincidences in the Theory of Brillouin Zones Lancaster Press, Lancaster, PA, 1937 Ph.d. thesis.
[5] E.I. Blount, Solid State Physics, 13 Academic Press, New York, 1962, p. 306.
[6] J. Zak, Berry's phase for energy bands in solids, Phys. Rev. Lett 62 (2747) (1989).
[7] G.P. Mikitik, Y.V. Sharlaĭ, J. Expt. Theor. Phys. JETP 87 (1998) 747.
[8] G.P. Mikitik, Y.V. Sharlaĭ, Manifestation of Berry's phase in metal physics, Phys. Rev. Lett. 82 (2147) (1999).
[9] G.P. Mikitik, Y.V. Sharlaĭ, Low. Temp. Phys. 33 (2007) 439.
[10] P.B. Allen, What happens to geometric phase when spin-orbit interactions lift band degeneracies?, 2007, arXiv:0709.1457.
[11] P.B. Allen, Accidental degeneracy and berry phase in simple band structures, 2007, presented at the CarFest Conference, Trieste, June 2007.
[12] M.V. Berry, Proc. R. Soc. Lond A 392 (1984) 45.
[13] M.V. Berry, Aspects of degeneracy, in: G. Casatil (Ed.), Chaotic Behavior in Quantum Systems, Plenum, New York, 1985, pp. 123–140.
[14] A.A. Burkov, M.D. Hook, L. Balents, Topological nodal semimetals, Phys. Rev. B 84 (235126) (2011).
[15] R.D. King-Smith, D. Vanderbilt, Theory of polarization of crystalline solids, Phys. Rev. B 47 (1651) (1993).
[16] R. Resta, Macroscopic polarization in crystalline solids: the geometric phase approach, Rev. Mod. Phys 66 (899) (1994).
[17] G. Sundaram, Q. Niu, Wave-packet dynamics in slowly perturbed crystals: Gradient corrections and berry-phase effects, Phys. Rev. B 59 (14915) (1999).
[18] F.D.M. Haldane, Berry curvature on the fermi surface: anomalous hall effect as a topological fermi-liquid property, Phys. Rev. Lett 93 (206602) (2004).
[19] A.M. Kosevich, Low. Temp. Phys. 30 (2004).
[20] K.S. Novoselov, A.K. Geim, S.V. Morosov, D. Jiang, M.I. Katsnelson, I.V. Grigorieva, S.V. Dubonos, A.A. Firsov, Nature 438 (2005) 197.
[21] Y. Zhang, Y.W. Tan, H.L. Stormer, P. Kim, Nature 438 (2005) 201.
[22] V. Pardo, W.E. Pickett, Electron confinement, orbital ordering, and orbital moments in $d^0 - d^1$ oxide heterostructures, Phys. Rev. B 81 (245117) (2010).
[23] C. Fang, Y. Chen, H.Y. Kee, L. Fu, Topological nodal line semimetals with and without spin-orbital coupling, Phys. Rev. B 92 (081201) (2015).
[24] M. Phillips, V. Ali, Tunable line node semimetals, Phys. Rev. B 90 (115111) (2014).
[25] T.T. Heikkilä, G.E. Volovik, Nexus and dirac lines in topological materials, New J. Phys 17 (093019) (2015).
[26] K. Mullen, B. Uchoa, D.T. Glatzhofer, Line of dirac nodes in hyperhoneycomb lattices, Phys. Rev. Lett 115 (026403) (2015).
[27] C. Fang, M.J. Gilbert, X. Dai, B.A. Bernivig, Multi-Weyl topological semimetals stabilized by point group symmetry, Phys. Rev. Lett. 108 (266802) (2012).
[28] S.M. Huang, A Weyl fermion semimetal with surface fermi arcs in the transition metal monopnictide TaAs class, Nat. Commun 6 (1) (2015).
[29] D.F. Xu, Y.P. Du, Z. Wang, Y.P. Li, X.H. Niu, Q. Yao, P. Dudin, Z.A. Xu, X.G. Wan, D. L. Feng, Chin. phys. lett, 2015, 32, 107101.
[30] B.Q. Lv, et al., Observation of Weyl nodes in TaAs, Nat. Phys. 11 (2015) 724–727.
[31] C. Shekhar, et al., Extremely large magnetoresistance and ultrahigh mobility in the topological Weyl semimetal candidate NbP, Nat. Phys 11 (645) (2015).
[32] H. Weng, C. Fang, Z. Fang, B.A. Berniveg, X. Dai, Weyl semimetal phase in non-centrosymmetric transition-metal monophosphides, Phys. Rev. X 5 (011029) (2015).
[33] K.H. Ahn, K.W. Lee, W.E. Pickett, Spin-orbit driven interaction collective electron-hole excitations in a noncentrosymetric nodal loop Weyl semimetal, Phys. Rev. B 92 (115149) (2015).
[34] Y. Sun, S.C. Wu, B. Yan, Topological surface states and fermi arcs of the non-centrosymmetric weyl semimetals TaAs, TaP, NbAs, and NbP, arXiv:1508.06649.
[35] L.X. Yang, Z.K. Liu, Y. Sun, H. Peng, H.F. Yang, T. Zhang, B. Zhou, Y. Zhang, Y.F. Guo, M. Rahn, D. Prabhakaran, Z. Hussain, S.K. Mo, C. Felser, B. Yan, Y.L. Chen, Weyl semimetal phase in the non-centrosymmetric compound TaAs, Nat. Phys 11 (728) (2015).
[36] Y. Quan, W.E. Pickett, Single nodal loop of degeneraies in minimal symmetry: triclinic $CaAs_3$, Phys. Rev. Lett 118 (176402) (2017).
[37] W. Bauhofer, M. Wittmann, H.G.v. Schnering, Structure, electrical and magnetic properties of $CaAs_3$, $SrAs_3$, $BaAs_3$, and EuP_3, J. Phys. Chem. Solids 42 (687) (1981).
[38] B. Oleš, H.G. von Schnering, Infrared studies of phonons and free carriers in $CaAs_3$, $SraAs_3$, $BaAs_3$, and α-EuP_3, J. Phys. C 14 (5559) (1981).